Spatial Low Frequency Pattern Analysis in Positron Emission Tomography: A Study Between Normals and Schizophrenics

Alejandro V. Levy, Francisco Gomez-Mont, Nora D. Volkow, Juan F. Corona, Jonathan D. Brodie, Robert Cancro

Nathan S. Kline Institute for Psychiatric Research, Orangeburg, New York, Department of Psychiatry, New York University School of Medicine, New York, New York, Unidad Informatica, Instituto Mexicano de Psiquiatria, Mexico City, Mexico, Medical Department, Brookhaven National Laboratory, Upton, Long Island, New York, Centro Cientifico, I.B.M. de Mexico, Mexico City, Mexico

Using the two-dimensional Fourier transform and the brain's centroidal principal axis, a method is developed for the analysis of PET metabolic brain images without the use of predefined anatomic regions of interest. We applied the method to images from a group of 11 normal and 12 medicated schizophrenics tested under resting conditions and under a visual task. A cortical/subcortical spatial pattern was found to be significant in two directions; anterior/posterior and chiasmatic (left-anterior/right-posterior). The best individual clinical classification (Jackknife classification) occurred under visual task at two axial brain levels: at the basal ganglia with correct classification rates of 91% and 84%, while the cerebellum had rates of 82% and 92%. These high classification rates were obtained using only the four coefficients of the lowest spatial frequency. These results point to the generalized brain dysfunction of regional glucose metabolism in chronic medicated schizophrenics both at rest and at a visual image-tracking task.

J Nucl Med 1991; 33:287–295

During the last 10 years, several methodologies have been proposed to analyze brain metabolic images obtained with positron emission tomography (PET). All of the methods developed to evaluate metabolic differences between brain task conditions or between patient groups can be classified into two global strategies; the traditional region of interest (ROI) and the new function of interest (FOI) strategy.

The ROI Strategy

One version of this strategy has been to compare brain regional metabolic differences between groups (*1–9*); another version has been to compare the pattern of metabolic interactions among brain areas between groups (*10–16*). Although these versions have been very useful in demonstrating metabolic changes in disease, they are limited by the fact that they require anatomical predefinition of the ROIs to be analyzed. For some research hypotheses, such as questions regarding a particular known pathway, this is the most appropriate protocol. However, if a pathway is not known a priori and only a few ROIs are selected, then these strategies might introduce a large source of error, since it has been shown that anatomical regions are functionally heterogeneous (*17*) and the PET metabolic images represent functional information.

The FOI Strategy

Recently, a second strategy has been developed by two research groups (*18–22,23–25*) that overcomes these limitations and analyzes the PET image of the whole brain without the need to define anatomical ROIs *a priori*.

In this strategy, once the functional image has been analyzed and significant neural patterns have been detected automatically by the method, then, *a posteriori*, these significant neural patterns are projected into an anatomical image and their anatomical ROI identification is obtained.

We have called this functional image-driven strategy the FOI strategy (*25*), to contrast its basic properties from those of the anatomical image driven ROI strategy. In the FOI strategy the use of a stereotactic anatomical atlas or a magnetic resonance brain image (MRI) comes at the end of the method, while in the ROI strategy the anatomical information is used in the first step of the method.

The FOI methods developed in (*18–22*) have used as a function of interest the PET difference image obtained by subtracting the resting brain image from a task-activated brain image of the same subject; this produces a different image with a small well defined focal region that was activated by the task. The projection of the activated region into a stereotactic anatomical brain atlas is obtained with the help of an additional lateral skull x-ray.

Received February 26, 1991; revision accepted September 19, 1991.
For reprints contact: A. V. Levy, PhD, Brookhaven National Laboratories, Upton, NY 11973.

The work done in (*23–25*) has used as a function of interest the PET image differences between clinical groups of normal and schizophrenic subjects; this produces a difference image with large complex patterns that extend throughout the brain pointing to those anatomical areas associated with the mental illness. These complex patterns are projected into a stereotactic anatomic atlas without the need of additional x-ray images; instead the brain's centroidal principal axis is extracted directly from the PET image.

Strategy of the Present Work

In this paper a method is presented for data synthesis and feature extraction of PET metabolic images from several clinical groups following the FOI strategy. However, the present method is not intended for the identification of functional-anatomical relationships. Its objective is to attain reliable clinical classification of a single subject in a practical way. This is done by achieving a large data compression ratio while retaining the meaningful features of the PET metabolic image. In a sense it is an extreme example of the FOI strategy since it only analyzes functional images; no anatomical data are ever used in the conclusions of the method.

In the present method, the original PET images are not used to compute a difference image as the FOI; instead a much simpler PET brain image is first obtained for each subject. These simpler images are easier to analyze and in spite of their reduced amount of data still retain the salient features that distinguish clinical groups and might even be used for clinical classification of a single subject. To obtain simpler meaningful images, we shall use a well-known technique for data compression whose geometric properties are now briefly presented.

A Geometric Interpretation of Two-Dimensional Fourier Transform (TDFT)

The TDFT is often used in image analyses (*26–28*) to represent any two-dimensional image as the sum of a set of simpler spatial patterns each one weighted by a Fourier coefficient. By applying TDFT, the thousands of numbers that are contained in a digital metabolic image can be represented by spatial patterns that retain the same basic geometric shape while their spatial frequency increases. Those Fourier coefficients associated with low spatial frequencies represent gross properties of the image; those associated with increasing spatial frequencies represent increasingly smaller image details (*29*).

A graphical representation of some of these simpler metabolic brain images is given in Figure 1, while some of the geometric patterns use by the TDFT are illustrated in Figure 2.

In this work, we are interested in comparing clinical groups of small size, with about 10 subjects per group. Therefore it is necessary to use a small number of variables as descriptors of each group. We have selected as descriptor variables the four coefficients related to the magnitude of

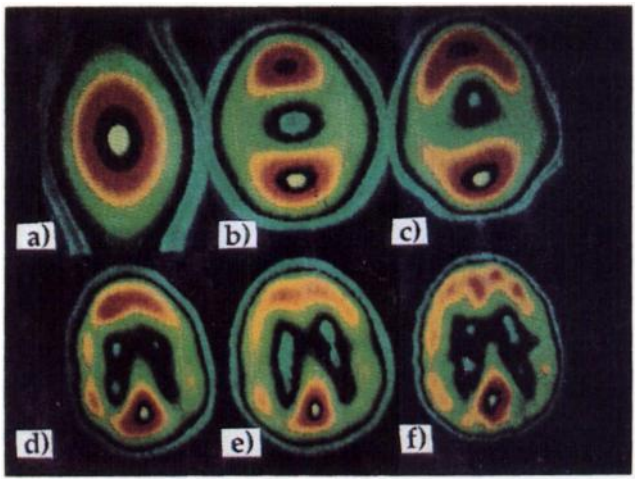

FIGURE 1. Simplified metabolic brain images obtained by TDFT by adding low spatial frequency (harmonic) patterns; (A) 0 and 1st harmonic, (B) 0, + 1st + 2nd harmonic, (C) 0 up to 3rd, (D) 0 up to 4th, (E) 0 up to 5th, (F) original PET VI brain metabolic image. The close approximation to (F) obtained by TDFT in (E), even if the 6th and higher spatial frequencies are not used, is possible because of the low spatial resolution in PET images; typically for a PET VI camera the FWHM is 11 mm. The original image has 5,184 numerical values, while (A) uses only 10 coefficient values, attaining a data compression ratio of 518.

the first spatial frequency normalized by the zero order coefficient, (the zero order Fourier coefficient is a single number that denotes the total metabolic activity of the slice). As shown in the Appendix, the resulting mathematical expressions for these four descriptor variables can be interpreted as feature descriptors for the brain's metabolic spatial patterns which contrast cortical/subcortical areas of the brain in four different directions: front/back, left/right and two chiasmatic ones; left-front/right-back, and right-front/left-back.

Since each brain slice image analyzed by TDFT consists of (72 × 72) pixels and each pixel represents 2.78 mm on its edge, then the first harmonic has a cycle of 2.78 mm × 72 or 20 cm per cycle. This study is therefore looking at just a few variables that represent the complex metabolic patterns contained in a PET image as a single large smooth metabolic pattern whose size is comparable to the size of the whole brain; this large smooth pattern is illustrated in Figure 3.

In the present method, we utilized TDFT for the characterization of the brain metabolic images because:

1. The geometrical shape and relative positions of the different brain structures, as described by the deoxyglucose method, reflects brain activity (*7,31,32*).
2. The analysis of PET images from various psychiatric populations has shown abnormal patterns of metabolism (*2,6,8,10,14*).
3. Higher cognitive functions and their disruptions in psychiatric disorders are not localized to a particular anatomical region but are widely distributed in the brain (*33–35*).

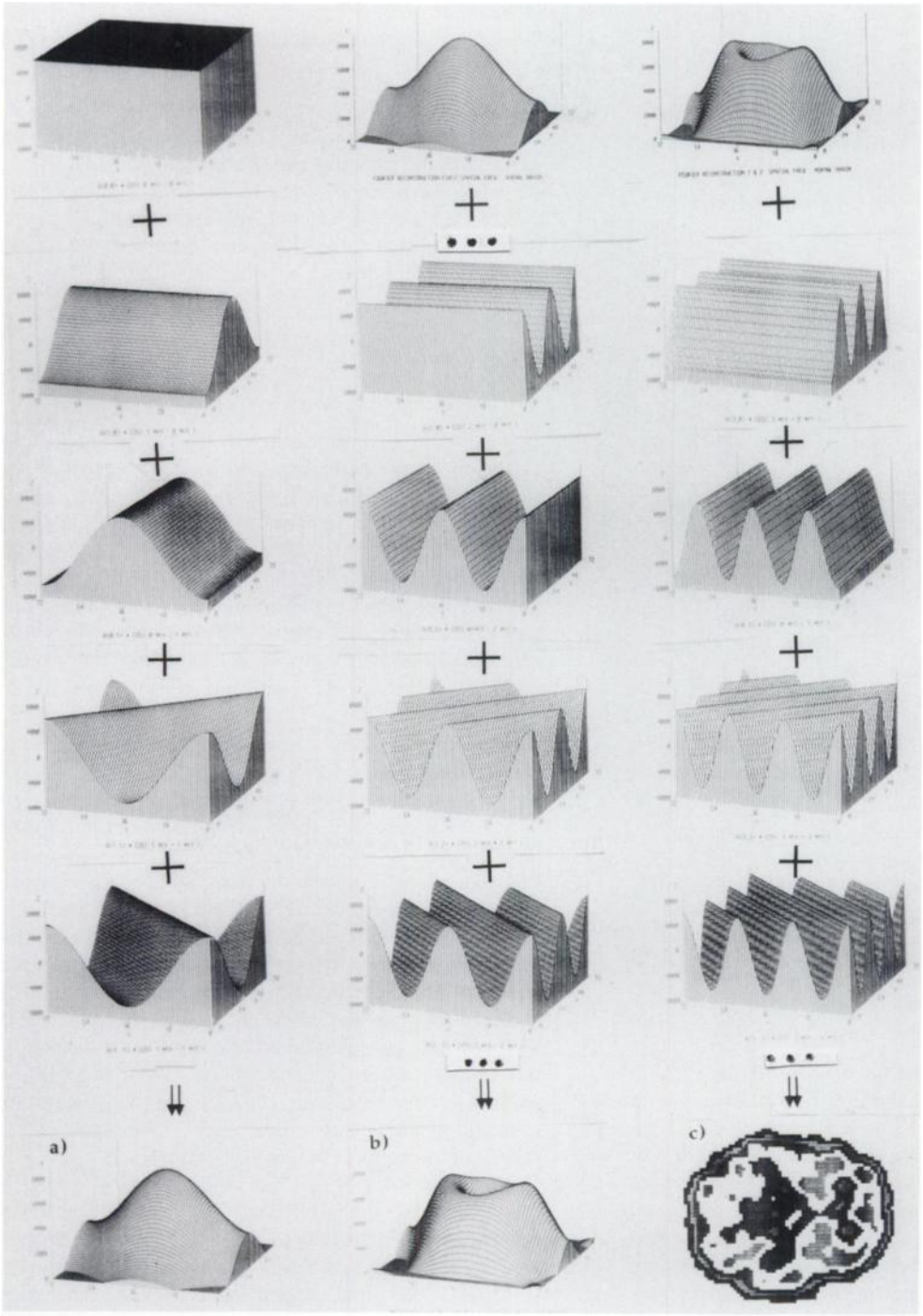

FIGURE 2. A few of the geometric patterns used by the TDFT to obtain the simplified brain images shown in Figure 1. Rows 2 to 5 illustrate the particular patterns in the front/back, left/right and chiasmatic directions as the spatial frequency increases from left to right. Figure 2A is obtained by adding the 0 and 1st harmonic patterns shown in the left hand column. As suggested in the middle column, Figure 2B is obtained as the second harmonic pattern is added to (A). As suggested in the right hand column, if all the patterns of the third and higher harmonics are added to (B), the TDFT would yield a better approximation to the original image, whose complex pattern is shown in Figure 2C.

4. All of the TDFT coefficients are computed using the metabolic information of the whole brain, therefore any one of these coefficients might be capable to characterize whole brain differences in clinical groups.

To test the validity of this method, we used the first harmonic (lowest frequency) coefficients from the TDFT of the metabolic images as a feature vector to discriminate between the metabolic patterns of images from control subjects and from schizophrenic patients.

Invariance of the Fourier Coefficients

In order to avoid the errors introduced in the TDFT coefficients because of positioning errors within the PET camera, we abandon the use of the image coordinates based in the reference axis of the camera.

Instead, we compute for each subject its unique, individual centroidal principal axis based on the geometric shape of its brain (*23,24,25*) and represent the brain image with coordinates in this invariant reference system. The sensitivity of the TDFT coefficients to intersubject head size is removed by scaling each brain slice to the common

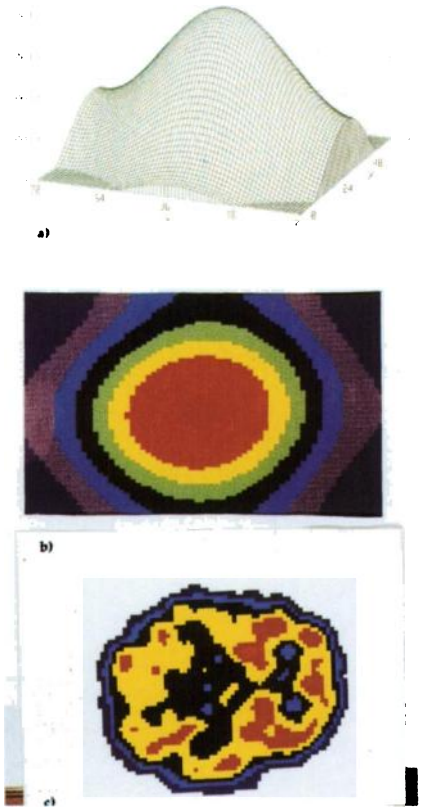

FIGURE 3. The small number of low frequency Fourier coefficients used in this study, represent the brain's metabolic activity as the smooth, large, spatial pattern shown in (A) and (B). The corresponding original metabolic PET brain image is shown in (C). The present study is able to identify a single subject as normal or schizophrenic with over 90% correct classification using only four normalized low frequency Fourier coefficients as feature descriptors of a complex metabolic PET brain image.

dimensions provided by Schaltenbrand's anatomic atlas (*30*).

MATERIALS AND METHODS

Scan Methodology

The positron emission scan was obtained using the PET-VI scanner at Brookhaven National Laboratory (FWHM resolution of 12 mm). Metabolic images were obtained using ^{11}C-deoxyglucose following a standard procedure as described elsewhere (*36*, *37*). The subjects were scanned twice on the same day, both under baseline conditions (eyes open, ears plugged) and upon activation with a visual eye-tracking task (*36*). While performing the studies, the room light was dim and noise kept to a minimum. A central sagittal and a canthomeatal line were used as references to align the laser beams. These same lines were used for repositioning of the subjects.

Subjects

The control group consisted of 11 right-handed males who were tested for absence of neurological or psychiatric abnormalities. The experimental group consisted of 12 right-handed male subjects who fulfilled DSM-III diagnostic criteria for schizophrenia. Clinical and demographic characteristics of the subjects have been described elsewhere (*36*).

Image Analysis

The images were reconstructed following a standard procedure (*37*). However, in order to make the Fourier coefficients insensitive to head size and head positioning within the PET camera, the following additional operations were performed on the PET images:

1. Automatic centering of the TDFT reference system on the centroidal and principal axis of the brain (*23–25*).
2. Rescaling the head size at each slice level by linear interpolation to that of Schaltenbrand's anatomic atlas (*30*).
3. Recoding of the image from the spatial domain to the spatial frequency domain by the TDFT.

The following statistical procedures were applied to the Fourier coefficients:

1. To determine if the differences in the Fourier coefficients characterizing the brain images of the control baseline and patient baseline groups are statistically significant, a one-way MANOVA was performed on the four TDFT coefficients of the two groups using procedure 4V from BMDP Statistical Software (*38*). The significance level, p, was tabulated for each of the 14 brain levels. Since 14 statistical tests were done, (one for each of the 14 brain slices), then according to Bonferroni's inequality the level that p must reach to attain statistical significance is reduced to 0.05/14 = 0.0035.
2. To determine if the differences in the Fourier coefficients characterizing the brain images of the two groups, control task and patient task, are statistically significant, the same procedure as described above in item 1 was performed on these groups.
3. Fourteen two-group linear discriminant analyses were performed using the procedure DISCRIM from the SAS Institute (*39*), 1 for each of the 14 slices using four variables. The two groups were: control baseline versus schizophrenia baseline. The percentile of the images correctly classified as either control baseline or patient baseline were tabulated. This statistical procedure was done again using the control task versus schizophrenia task groups. Also, in order to give an idea of the separation between the two groups, the generalized Mahalanobis distance was computed by the DISCRIM procedure (*39*) for each brain level.
4. To determine if a single individual, could be correctly classified by the four TDFT coefficients as either control baseline or patient baseline, 1 subject was removed from its group and 14 2-group linear discriminant analyses were performed (*39*), 1 for each of the 14 brain slices. Since there are 23 subjects at baseline, a total of $23 \times 14 = 322$ two-group discriminant analyses were performed. Once the discriminant function coefficients have been computed, the subject that was left out of the computations is classified in either group. The percentile of true classifications achieved by each brain level was tabulated as a "Jackknife true classification rate" (*40,41*).
5. To determine if a single individual could be correctly classified by the four TDFT coefficients as either control task or patient task, one subject was removed from its group and a similar procedure as described in item 4 above was performed. The percentile of true classifications achieved by each brain level was tabulated as a "Jackknife true classification rate."

RESULTS

Multiple Analysis of Variance

Table 1 shows the statistical significance level, p, computed from a one-way MANOVA for each of the brain levels. These results show that the differences between the Fourier coefficients of controls and schizophrenics, both at base line, reach low p values in five contiguous brain slices and are statistically significant ($p < 0.0035$) at the levels of the thalamus and basal ganglia.

The MANOVA results in the case of the control and schizophrenic groups, both under task, indicate that the Fourier coefficients of three contiguous slices in the thalamus and basal ganglia and one slice at the cerebellum have low p values. The basal ganglia level reaches statistical significance at the $p < 0.0035$ value.

Spatial Asymmetries in Brain Metabolic Activity

The MANOVA procedure (*38*) also indicates results for the statistical significance in a pairwise univariate comparison for each of the four Fourier coefficients.

As shown in Figure 2 and mathematically described in the Appendix, each of the 1st harmonic Fourier coefficients can be associated with a cortical/subcortical pattern that performs a directional sampling in four spatial directions. The Fourier coefficient associated with the anterior/posterior spatial direction has a very high statistical significance in the thalamus and basal ganglia, reaching a value $p < 0.00009$ at level 8. The Fourier coefficient associated with the cortical/subcortical contrast of metabolic activity in a chiasmatic left anterior/right posterior spatial direction has statistical significance at the level of the basal ganglia with a value of $p < 0.003$.

TABLE 1
MANOVA Statistical Significance Analysis

	Resting	Visual tracking
Brain level	p	p
1 Superior C.S.	0.37	0.59
2 Superior C.S.	0.89	0.28
3 C.S.	0.62	0.11
4 C.S.	0.12	0.19
5 Inferior C.S.	0.21	0.56
6 Inferior C.S.	0.04	0.17
7 Thalamus	0.02	0.38
8 Thalamus	0.001*	0.006
9 Basal ganglia	0.02	0.003*
10 Basal ganglia	0.001*	0.008
11 O.F.G.	0.17	0.13
12 O.F.G.	0.23	0.20
13 Cerebellum	0.53	0.01
14 Cerebellum	0.19	0.27

Level of statistical significance p, obtained from a MANOVA test contrasting the 4 Fourier coefficients that characterize each of the 14 brain levels in the normal (n = 11) and schizophrenic (n = 12) groups.
C.S. = centrum semiovale and O.F.G. = orbito-frontal gyrus.
* Differences between the two groups are statistically significant ($p < 0.0035$).

TABLE 2
Two–Group Discriminant Analysis

	Resting		Visual Tracking	
	Normals	Schizophrenics	Normals	Schizophrenics
Brain level	% correct	% correct	% correct	% correct
1	73	67	70	75
2	67	57	75	73
3	58	73	92	80
4	83	87	67	73
5	75	64	75	79
6	73	64	82	67
7	75	93	67	80
8	92*	100*	92*	93*
9	92	60	83	87
10	83	93	83	87
11	67	67	58	67
12	70	80	60	80
13	64	93	82*	100*
14	80	70	70	73

% correct are the number of subjects in each group of normals (n = 11) and schizophrenics (n = 12) correctly classified.
* Brain level (thalamus and cerebellum) with an outstanding group classification rate.

Two-Group Discriminant Analysis

Table 2 presents the results of the two-group discriminant function analyses that were performed on each of the 14 anatomical levels.

Table 2 (left side) shows the correct classification rates between control and schizophrenic baselines; the correct classification rate varies from 57% to 100% in the schizophrenics and from 58% to 92% in the normals for the different slices. The best separation between normals and schizophrenics is obtained in the images at level 8, where the basal ganglia and thalamus are located with correct classification rates of 92% and 100%.

Table 2 (right side) also shows the correct classification rates between control and schizophrenic tasks; the correct classification rate varies from 60% to 92% in the normals and from 67% to 100% in the schizophrenics for the different slices. The best classification between normals and schizophrenics is obtained in the images at level 8, where the basal ganglia and thalamus are located with correct classification rates of 92% and 93%. The visual tracking task has activated the cerebellum, which at level 13 attains a correct classification rate of 82% and 100%.

"Jackknife" Single-Subject Discriminant Analysis

Table 3 presents the results of the "Jackknife" single-subject linear discriminant function analyses that were performed on each of the fourteen anatomical levels.

It shows that the Jackknife true classification rate for a single control subject at rest varies from 27% to 75% and for a schizophrenic at rest it varies from 23% to 85%. For subjects under task, the true classification rate for a control

TABLE 3
Single Subject Discriminant Analysis ("Jackknife")

Brain Level	Resting		Visual Tracking	
	Normals	Schizophrenics	Normals	Schizophrenics
	% correct	% correct	% correct	% correct
1	45	50	44	33
2	27	23	64	57
3	45	71	64	64
4	66	85	54	64
5	58	57	54	54
6	54	61	50	57
7	50	71	64	57
8	75*	85*	91*	84*
9	66	71	82	64
10	66	71	91	71
11	50	57	54	64
12	60	64	44	64
13	58	71	82*	92*
14	54	41	70	60

% correct is the number of times an individual subject removed from the group of normals (n = 11) or schizophrenics (n = 12) was classified correctly.

* Brain level (thalamus and cerebellum) with an outstanding subject classification rate.

subject ranges from 44% to 91%, and for a schizophrenic subject, it varies from 33% to 92%.

The best classification under resting conditions between normals and schizophrenics is obtained in the images at level 8, where the basal ganglia are located with correct classification rates of 75% and 85%. Under the visual tracking task, the best classification is obtained at two levels. Level 8 containing the basal ganglia has correct classification rates of 91% and 84% and level 13 which now has an activated cerebellum that attains correct classification rates of 82% and 92%.

It is important to point out that according to Gray and Schucany and James (*40,41*) these classification rate results are non-parametric measures of the separability of two groups in feature space, since the Jackknife method does not require normality or any other statistical conditions on the feature variables.

Mahalanobis Distance

To geometrically illustrate the relative distance in feature space between the normal and schizophrenic groups, the generalized Mahalanobis distance was also computed by the procedure DISCRIM (*39*).

This procedure computes the "generalized distance" (Mahalanobis distance), between two groups using as "units of distance" a unit related to the spread of each group, i.e., the group's covariance matrix. Let the feature variables (in this study, the four normalized TDFT coefficients) in group 1 have a mean X_1, let group 2 have a mean X_2, and denote the covariance matrix by $[\Sigma]$.

The formula $(D_{1,2})^2 = (X_1 - X_2)^t[\Sigma]^{-1}(X_1 - X_2)$ is used by the procedure DISCRIM, yielding a "generalized distance" proportional to the distance between the means and inversely proportional to the group's spread about their means. Here $(X_1 - X_2)$ denotes a four-dimensional vector, $(\,)^t$ denotes its transpose, and $[\,]^{-1}$ denotes the inverse of the matrix.

As shown in Figure 4A, for resting conditions the Mahalanobis distance increases from low values at the top and bottom of the brain, levels 1 and 14, at its maximum value for level 8, which contains the lower thalamus and upper basal ganglia. As shown in Figure 4B, for the groups under the visual tracking task, the cerebellum at level 13 is activated in such a way that its Mahalanobis distance becomes as large as that of the lower thalamus and the basal ganglia at levels 8, 9, and 10.

It is important to point out that according to James (*41*) these Mahalanobis distance results are a non-parametric measure of the separability of two groups in feature space, since this generalized distance $(D_{1,2})$ does not require normality or any other statistical conditions on the feature variables.

DISCUSSION

Quantitative image analysis aims to obtain a set of numbers that reflect in a parsimonious manner some important properties of the structure being studied. Usually, these numbers reflect lengths, areas, volumes or averages across sets of pixels within an anatomical ROI. The

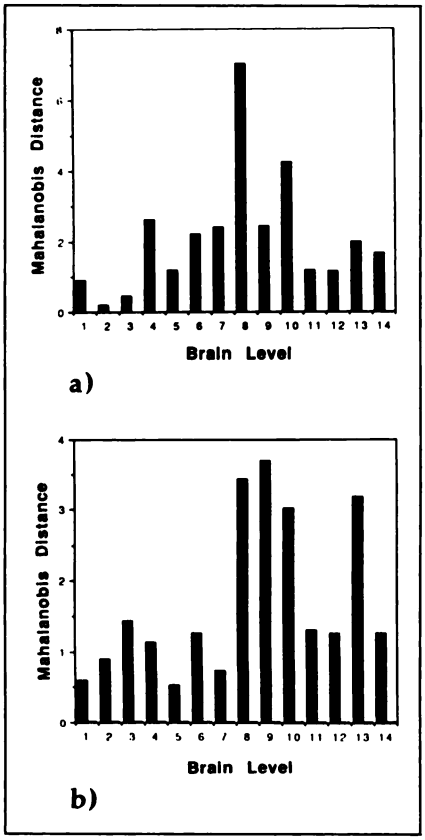

FIGURE 4. Mahalanobis distance between the normal and schizophrenic groups in feature space, computed with the four normalized first harmonic Fourier coefficients: (A) both groups at rest and (B) both groups under a visual tracking task. Level 1 is at the top of the brain. The brain levels showing the largest group differences are (A) brain levels 8 and 10 containing the lower thalamus and basal ganglia and (B) brain levels 8, 9, and 10 containing the thalamus and basal ganglia, plus the cerebellum at level 13 which has become activated by the visual tracking task.

TDFT can be seen as an alternative and complementary method for the automatic analysis of PET images, where the ROI is the entire image, and periodic structures and symmetry patterns are quantified. By applying TDFT, the information from the metabolic image can be represented as a set of Fourier coefficients (*29*).

It is well known that the Fourier coefficients of an image are sensitive to translations and rotations of the image. To avoid this sensitivity to the positioning of the subject's head within the PET camera, we abandon the PET camera coordinate axis and define the PET brain image in terms of the brain's centroidal principal axis (*23–25*), which is unique to each brain and insensitive to head positioning variations. To avoid the sensitivity of the Fourier coefficients to the size of the PET brain images, they are scaled to a unique brain size (*23,25*) given by a stereotactical anatomical atlas (*30*).

The good clinical group discrimination obtained with the first harmonic of this analytical technique documents its capacity to represent salient gross features of metabolic brain images adequately. It also shows that the analyses of global geometrical characteristics of an image, as opposed to its anatomical partitions, is of value in the detection of functional patterns that can distinguish control from psychiatric groups. Furthermore, this procedure can obtain the normal/schizophrenic classification of individual subjects from PET images in a highly significant fashion, without subjective decisions about which anatomical ROI are selected for the classification.

The results derived from the analysis of the global properties of the metabolic activity showed several characteristics that merit further interpretation. One is the widespread nature of the discriminating power of the Fourier variables in differentiating normal subjects from psychiatric patients. This was shown by the good discrimination obtained across several anatomical levels while using only the global spatial coverage of the first harmonic. The anatomical level where the differences were most marked was at the level of the basal ganglia. This is an area rich in dopamine receptors and has been implicated in the pathophysiology of mental illness (*42*).

The physiological/anatomical representation of the normalized Fourier coefficients for the first harmonic as used in this method is a contrast function between the cortical/subcortical metabolic activity along four directions: front/back, left/right and two chiasmatic (left anterior/right posterior and right anterior/left posterior). Previous studies using the ROI approach have also documented abnormal frontal activity in schizophrenic subjects using PET to measure glucose metabolism and using ^{133}Xe to measure cerebral blood flow (*4,14,43*). The replication of this finding across different techniques and groups of patients suggests that the association between anterior/posterior and cortical/subcortical brain areas represents a basic interaction pattern of brain activity.

The Fourier analysis also shows a chiasmatic (left-anterior/right-posterior) interaction that distinguishes normal subjects from schizophrenic patients. This axis has been related to psychopathology in anatomical studies done both in schizophrenia and in autism (*45,46*).

The activation of the cerebellum under the visual tracking task was an unexpected result that merits further analysis. The preliminary results of this additional study using the traditional ROI approach is underway; preliminary results can be found in the Volkow et al. study (*47*).

In interpreting these results, one has to exclude the effects of neuroleptics in brain glucose metabolism, since the schizophrenic patients studied here have all been under several years of treatment. Longitudinal prospective studies are needed in order to address this issue, and we cannot conclude that these observations are not due in part to the effects that neuroleptics might have on brain organization.

Like other FOI methods, the analysis of the spatial frequency pattern avoids the use of predefined anatomical regions, eliminates the subjective drawing of anatomical boundaries and avoids averaging metabolic rates within an anatomical region. It has the advantage of reflecting global geometrical properties of each image with just a few numbers. This strategy also allows itself to three-dimensional Fourier analyses of PET metabolic images, thus providing a method for investigating functional activity of the brain as a whole.

On the other hand, direct anatomical interpretation of the spatial patterns obtained by the present method is not possible. Two FOI methods that have the capability to identify automatically anatomical ROIs a posteriori can be found in references (*18–22*) and (*24,25*).

In general, it is important to note the complementary value of FOI methods to ROI methods: once a FOI method has determined the spatial location of the significant brain patterns, a simpler practical computer implementation might be possible by taking advantage of this spatial information using the detected significant ROIs in a traditional ROI strategy that might be already available to the user.

In particular, one can implement the present method in a simpler way, thus achieving a reduction in computation time while avoiding the effort involved in drawing the ROIs: since only the 0 and 1st harmonic coefficients are needed by the method, the complete TDFT is not really required and as indicated by Dahlquist and Acton (*48,49*) these few coefficients can be obtained by simple summation formulas. This brings the computing effort to a level similar to that of computing the weighted sum of metabolic activity in one subcortical and four cortical areas, or to the level of computing the brain's metabolic centroid (*23*) which takes 0.3 sec on a main frame computer and a few seconds on a smaller PC.

CONCLUSION

In conclusion, the data reported here indicate the utility of the first spatial frequency of PET metabolic images as shown by its ability to discriminate adequately individual

subjects across normals and schizophrenics. This, plus the significant discrimination observed between the clinical groups at the thalamus, basal ganglia, and cerebellum using only the large spatial brain pattern associated with the first spatial frequency harmonic, point to the widespread nature of the differences between normals and schizophrenics and give evidence for the nonlocalized nature of abnormalities in brain glucose metabolism of chronic medicated schizophrenic patients.

In a broader perspective, the unexpected emergence of a functionally different cerebellum in the schizophrenic group when performing a visual tracking task points to a successful general strategy for exploring the differences between normal and mentally ill brains; by imposing a task that stresses the system, the weakest link is extracted from a highly complex mechanism.

APPENDIX

TDFT can be used to represent an image F(x, y) contained inside a rectangle of dimensions $-p/2 < x < p/2$ and $-q/2 < y < q/2$ as a sum of cosine functions. If only the zero and first spatial frequency are used to approximately represent the image F(x, y) as F′(x, y), then the image is given in terms of the magnitude $C_{j,k}$ and phase angle $\Theta_{j,k}$ of the cosine functions by the following expression

$$F'(x, y) = C_{0,0} + 2C_{1,0}\cos(2\pi Ux + \Theta_{1,0}) + 2C_{0,1}\cos(2\pi Vy + \Theta_{0,1}) + 2C_{1,1}\cos(2\pi Ux + 2\pi Vy + \Theta_{1,1}) + 2C_{1,-1}\cos(2\pi Ux - 2\pi Vy + \Theta_{1,-1})$$

where $U = 1/p$ and $V = 1/q$.

The directional characteristic of each term of this equation is graphically illustrated in the left hand column of Figure 2, by the spatial patterns of cos(x), cos(y), cos(x + y), and cos(x − y). These functions attain positive values (0, 1) in the central areas of the brain and mostly negative values (0, −1) at the brain's edge.

In the present method, we shall use the four TDFT normalized Fourier coefficients $C_{1,0}/C_{0,0}$, $C_{0,1}/C_{0,0}$, $C_{1,1}/C_{0,0}$ and $C_{1,-1}/C_{0,0}$, which contrast the brain's central areas to its edge areas in the four directions left/right, front/back, right frontal/left back and left frontal/right back, respectively. By taking as a reference $C_{0,0}$, which is the value of the total metabolic activity in the brain slice, the relative importance of each directional pattern is enhanced.

ACKNOWLEDGMENTS

The authors wish to thank J. Fowler, K. Karlstrom, and A. Farrell for preparation of the labeled deoxyglucose; D. Christman for data acquisition; J. Casillas and E. Gutierrez for data processing; L. Martinez-Negrete, M. Hernandez, M. Meisner, and H. B. Kushner for mathematical and statistical consultation; and P. van Gelder for performing the visual stimulation/motor activation task.

This work was supported in part by NIMH grant MH44832, the U.S. Department of Energy under contract no. DE-AC02-76CH00016, U.S. NIH grant NS 15638 from the NINCDS, the Nathan S. Kline Institute for Psychiatric Research, the Mexican Institute of Psychiatry, and the Scientific Center of I.B.M. in Mexico City. A preliminary report of this work was presented at the 37th Annual Meeting of Society of Nuclear Medicine, Washington DC, June 19–22, 1990.

REFERENCES

1. Phelps ME, Huang SC, Hoffman EJ, Selin C, Sokoloff L, Kuhl DE. Tomographic measurement of local cerebral glucose metabolic rate in humans with [^{18}F]2-fluoro-2-deoxy-D-glucose. Validation of method. *Ann Neurol* 1979;6:371–388.
2. Buchsbaum MS, Wu JC, DeLisi LE, et al . Positron emission tomography studies of basal ganglia and somatosensory cortex neuroleptic drug effects: differences between normal controls and schizophrenic patients. *Biol Psychiatry* 1987;22:479–494.
3. Mazziotta JC, Phelps ME, Carson RE, Kuhl DE. Tomography mapping of human cerebral metabolism: auditory stimulation. *Neurology* 1982;32:921–937.
4. Buchsbaum MS, Ingvar DH, Kessler R, et al. Cerebral glucography with positron tomography. *Arch Gen Psych* 1982;39:251–259.
5. Patronas NJ, DiChiro G, Brooks RA, et al. Work in progress: [^{18}F] fluorodeoxyglucose and positron emission tomography in the evaluation of radiation necrosis of the brain. *Radiology* 1982;144:885–889.
6. Duara R, Grady C, Haxby J, Sundaram M, et al. Positron emission tomography in Alzheimer's disease. *Neurology* 1986;36:879–887.
7. Greenberg JH, Reivich M, Alan A, et al. Metabolic mapping of functional activity in human subjects with the [^{18}F]fluorodeoxyglucose technique. *Science* 1981;212:678–680.
8. Haxby JV, Duara R, Grady CL, Cutler NR, Rapaport SI. Relations between neuropsychological and cerebral metabolic asymmetries in early Alzheimer's disease. *J Cereb Blood Flow Metab* 1985;5:193–200.
9. Young AB, Penney JB, Starosta-Rubinstein S, et al. PET scan investigations of Huntington's disease: cerebral metabolic correlates of neurological features and functional decline. *Ann Neurol* 1986;20:296–303.
10. Clark CM, Kessler R, Buchsbaum MS, Margolin RA, Holcomb HH. Correlational methods for determining regional coupling of cerebral glucose metabolism: a pilot study. *Biol Psych* 1984;19:663–678.
11. Horwitz B, Duara R, Rapaport SI. Age differences in intercorrelations between regional cerebral metabolic rates for glucose. *Ann Neurol* 1986;19:60–67.
12. Metter EJ, Reige WH, Kuhl DE, Phelps ME. Cerebral metabolic relationships for selected brain regions in healthy adults. *J Cereb Blood Flow Metab* 1984;4:1–7.
13. Metter EJ, Reige WH, Kamayema M, Kuhl DE, Phelps ME. Cerebral metabolic relationships for selected brain regions in Alzheimer's, Huntington's, and Parkinson's disease. *J Cereb Blood Flow Metab* 1984;4:500–506.
14. Volkow ND, Brodie JD, Wolf AP, et al. Brain organization in schizophrenia. *J Cereb Blood Flow Metab* 1986;6:441–446.
15. Moeller JR, Strother SC, Sidtis JJ, Rottenberg DA. Scaled subprofile model: a statistical approach to the analysis of functional patterns in positron emission tomographic data. *J Cereb Blood Flow Metab* 1987;7:649–658.
16. Volkow ND, Brodie JD, Wolf AP, Angrist B, Russel JAG, Cancro R. Brain metabolism in schizophrenics before and after acute neuroleptic administration. *J Neurol Neurosurg Psychiatry* 1986;49:1199–1202.
17. Sheider JS. Basal ganglia role in behavior. Importance of sensory gating and its relevance to psychiatry. *Biol Psych* 1984;29:1693–1710.
18. Fox PT, Perlmutter JS, Raichle ME. A stereotactic method of anatomical localization for positron emission tomography. *J Comp Assist Tomogr* 1985;9:141–153.
19. Fox PT, Mintum MA, Raichle ME, Miezin FM, Allman JM, Van Essen DC. Mapping of human visual cortex with positron emission tomography. *Nature* 1986;332:806–809.
20. Fox PT, Mintum MA, Reiman EM, Raichle ME. Enhanced detection of focal brain responses using intersubject averaging and change distribution analysis of substracted PET images. *J Cereb Blood Flow Metab* 1988;8:642–653.
21. Mintum MA, Fox PT, Raichle ME. A highly accurate method of localizing regions of neuronal activation in the human brain with positron emission tomography. *J Cereb Blood Flow Metab* 1989;9:96–103.
22. Fox PT, Miezin FM, Allman JM, Van Essen DC, Raichle ME. Retinotopic organization of human visual cortex mapped with positron emission tomography. *J Neurosci* 1987;7:913–922.
23. Levy AV, Brodie JD, Russel JAG, Volkow ND, Laska E, Wolf AP. The

metabolic centroid method for PET brain image analysis. *J Cereb Blood Flow Metab* 1989;9:388–397.
24. Levy AV, Volkow ND, Brodie JD, Bertollo DN, Wolf AP. The spectral analysis of brain glucose metabolism. *Proc. 12th Int. Conf. IEEE in Medicine and Biology Society,* Philadelphia, PA, Nov 1–4. 1990;12:1299–1302.
25. Levy AV, Laska E, Brodie JD, Volkow ND, Wolf AP. The spectral signature method for the analysis of PET brain images. *J Cereb Blood Flow Metab* 1991;11:A103–A113.
26. Tallman OH. The classification of visual images by spatial filtering (dissertation). Air Force Institute of Technology, School of Engineering, June 1969.
27. Granlund G. Recognition of letters with Fourier methods. *IEEE Computing Group Repository Paper* 1970;R-70-98.
28. Andrews HC. Multidimensional rotations in feature selection. *IEEE Trans Computers* 1971;20:1045–1051.
29. Brigham EO. *The fast Fourier transform.* Englewood Cliffs, NJ: Prentice Hall, 1974.
30. Schaltenbrand G, Wharen W. *Atlas for stereotaxy of the human brain.* Chicago: Year Book Publishers; 1977: Plates 7, 11.
31. Schwartz EL. Anatomical and physiological correlates of visual computation from striate to infero-temporal cortex. *IEEE Trans Systems Man Cybern* 1984;14:257–271.
32. Sokoloff L, Reivich M, Kennedy C. The [^{14}F]fluorodeoxyglucose method for the measurement of local cerebral glucose utilization: theory, procedure and normal values in the conscious and anesthetized albino rat. *J Neurochem* 1977;28:897–916.
33. Livanov MN. *Spatial organization of cerebral processes.* New York, NY: Wiley; 1977.
34. Luria AR. *The working brain.* Translated by Haigh B. New York, NY: Baru Books; 1961.
35. Volkow ND, Tancredi LR. Biological correlates of mental activity studied with PET. *Am J Psych* 1991;4:439–443.
36. Volkow N, Van Gelder P, Wolf AP, et al. Phenomenological correlates of metabolic activity in chronic schizophrenics. *Am J Psych* 1987;144:151–158.
37. Reivich M, Alavi A, Wolf A, et al. Glucose metabolic rate kinetic model parameter determination in man. The lumped constants and rate constants for ^{18}F-fluorodeoxyglucose and ^{11}C-deoxyglucose. *J Cereb Blood Flow Metab* 1985;5:179–192.
38. BMDP Statistical Software Inc. Los Angeles, CA 90025.
39. SAS Institute Inc., Box 8000, Cary, NC 27512-8000, USA.
40. Gray HL, Schucany WR. *The generalized Jackknife statistic.* New York, NY: Marcel Dekker Inc. 1972:120–125.
41. James M. *Classification algorithms.* New York, NY: John Wiley & Sons. 1985:56–57.
42. Lidsky TI, Weinhold PM, Levine FM. Implications of basal ganglionic dysfunction for schizophrenia. *Biol Psych* 1979;14:3–12.
43. Farkas T, Wolf AP, Jaeger J, et al. Regional brain glucose metabolism in chronic schizophrenia. *Arch Gen Psych* 1984;41:293–300.
44. Ingvar DH, Franzen G. Distribution of cerebral activity in chronic schizophrenics. *Lancet* 1974;2:1484–1486.
45. Hier DB, LeMay M, Rosenberger PB. Autism: association with reversed cerebral symmetry. *Neurol* 1978;28:348–349.
46. Luchine DJ, Weinberger SR, Wyatt RJ. Schizophrenia: evidence of a subgroup with reversed cerebral symmetry. *Arch Gen Psych* 1979;36:1309–1311.
47. Volkow ND, et al. Decreased cerebellar metabolism in chronic medicated schizophrenics. Internal Report, Medical Department, Brookhaven National Laboratory, 1991.
48. Dahlquist G, Bjorck A. *Numerical methods.* Englewood Cliffs, NJ: Prentice Hall, 1974:405–412.
49. Acton FS. *Numerical methods that work.* New York: Harper and Row, 1970:228–233.